Inorg. Chem. **2006**, *45*, 4706–4711

Synthesis and Crystal Chemistry of Two New Fluorite-Related Bismuth Phosphates, $Bi_{4.25}(PO_4)_2O_{3.375}$ and $Bi_5(PO_4)_2O_{4.5}$, in the Series $Bi_{4+x}(PO_4)_2O_{3+3x/2}$ ($0.175 \leq x \leq 1$)

B. Muktha and T. N. Guru Row*

Solid State and Structural Chemistry Unit, Indian Institute of Science, Bangalore 560012, India

Received January 23, 2006

Two new phosphates, $Bi_{4.25}(PO_4)_2O_{3.375}$ and $Bi_5(PO_4)_2O_{4.5}$, have been analyzed by single-crystal X-ray diffraction in the series $Bi_{4+x}(PO_4)_2O_{3+3x/2}$ ($0.175 \leq x \leq 1$). The syntheses of the compositions ranging from $x = 0.175$ to 0.475 were carried out by the ceramic route. The compositions from $x = 0.175$ to 0.475 form a solid solution with a structure similar to that of $Bi_{4.25}(PO_4)_2O_{3.375}$, while $Bi_5(PO_4)_2O_{4.5}$ was isolated from a mixture of two phases. Both of the phases form fluorite-related structures but, nevertheless, differ from each other with respect to the arrangement of the bismuth atoms. The uniqueness in the structures is the appearance of isolated PO_4 tetrahedra separated by interleaving $[Bi_2O_2]$ units. ac impedance studies indicate conductivity on the order of 10^{-5} S cm^{-1} for $Bi_{4.25}(PO_4)_2O_{3.375}$. Crystal data: $Bi_{4.25}(PO_4)_2O_{3.375}$, triclinic, space group $P\bar{1}$ (No. 1), with $a = 7.047(1)$ Å, $b = 9.863(2)$ Å, $c = 15.365(4)$ Å, $\alpha = 77.604(4)°$, $\beta = 84.556(4)°$, $\gamma = 70.152(4)°$, $V = 980.90(4)$ Å^3, and $Z = 4$; $Bi_5(PO_4)_2O_{4.5}$, monoclinic, space group $C2/c$ (No. 15), with $a = 13.093(1)$ Å, $b = 5.707(1)$ Å, $c = 15.293(1)$ Å, $\beta = 98.240(2)°$, $V = 1130.95(4)$ Å^3, and $Z = 8$.

Introduction

δ-Bi_2O_3 (the high-temperature cubic form) exhibits good ionic conductivity due to the disorder in the oxygen substructure of the fluorite-type structure.[1−3] δ-Bi_2O_3 is stable only between 973 and 1097 K, and extensive literature deals with the stabilization of this phase at room temperature by substitution of various metal oxides. The $Bi_2O_3-P_2O_5$ system has been explored for this purpose, and it is interesting to note that $Bi_2(PO_4)_2$ itself crystallizes in two modifications. The room-temperature form is of the monazite structural type, which upon heating to 750 °C transforms to a second monoclinic polymorph.[4] Volkov et al. investigated the $Bi_2O_3-Bi_2(PO_4)_2$ system in detail and have identified four compounds at room temperature with ratios of 11:9, 12:13, 1:2, and 3:8 $Bi_2O_3-Bi_2(PO_4)_2$ and three compounds at high temperature in the ratios 1:1, 5:7, and 2:7 of $Bi_2O_3-Bi_2(PO_4)_2$.[5] The sillenite-type solid solution of the Bi_2O_3-rich part of the system was extensively studied owing to their electrical properties.[6,7] Also, substitution of V for P in $Bi_7P_{1-y}V_yO_{13}$ has been observed to significantly enhance ionic conductivity ($\sim 10^{-1}$ S cm^{-1}).[8]

Fluorite-related structure types in the $Bi_2O_3-P_2O_5$ system represent some of the highly conducting oxides. The large compositional range $Bi_{18-4x}(MO_4)_{4x}O_{27-12x}$ ($0 \leq x \leq 1$; M = P, V) has been studied by Darriet et al.[9] They found for $x = {}^2/_3$ a fluorite-type superstructure with $3 \times 3 \times 3$ subcells. The compound $Bi_{15.33}(MO_4)_{2.667}O_{19}$ (or $Bi_{46}(PO_4)_8O_{57} \equiv Bi_{11.5}(PO_4)_2O_{14.25}$ in our notation) can be described by stacking of $Bi_{14}(MO_4)_4O_{15}$ ($x = 1$) and $Bi_{18}O_{27}$ ($x = 0$) layers along the monoclinic c axis. In this case, the $x = 1$ and 0 layers are in the ratio 2:1, giving the general formula $x = {}^2/_3$ for the compound. Darriet et al. assume that the oxygen conductivity is related to partially occupied oxygen positions

* To whom correspondence should be addressed. E-mail: ssctng@sscu.iisc.ernet.in. Tel: +91-80-22932796 or +91-80-22932336. Fax: +91-80-23601310.

(1) Gattow, G.; Schröder, H. Z. *Z. Anorg. Allg. Chem.* **1962**, *318*, 176.
(2) Harwig, H. A. *Z. Anorg. Allg. Chem.* **1978**, *444*, 151.
(3) Takahashi, T.; Iwahara, H. *Mater. Res. Bull.* **1978**, *13*, 1447.
(4) Romero, B.; Bruque, S.; Aranda, M. A. G.; Iglesias, J. E. *Inorg Chem.* **1994**, *33*, 1869.
(5) Volkov, V. V.; Zhereb, L. A.; Kargin, F.-Y.; Skorikov, V. M.; Tanaev, I. V. *Russ. J. Inorg Chem.* **1983**, *28*, 1002.
(6) Watanabe, A.; Komada, H.; Takenouchi, S. *J. Solid State Chem.* **1990**, *85*, 76.
(7) Wignacourt, J. P.; Drache, M.; Conflant, P.; Boivin, J. C. *J. Chim. Phys.* **1991**, *88*, 1939.
(8) Wignacourt, J. P.; Drache, M.; Conflant, P. *J. Solid State Chem.* **1993**, *105*, 44.
(9) Darriet, J.; Launay, J. C.; Zúniga, F. J. *J. Solid State Chem.* **2005**, *178*, 1753.

10.1021/ic0601337 CCC: $33.50
Published on Web 05/16/2006

in the $Bi_{18}O_{27}$ layers. This is supported by the fact that $Bi_{14}(MO_4)_4O_{15}$ is not a good conductor[10] and that a study of the series $Bi_{46}(V_{1-x}P_xO_4)_8O_{57}$ ($0 \le x \le 1$) shows good conductivity for all investigated compounds, indicating that substitution of V for P in the $Bi_{14}(MO_4)_4O_{15}$ layers does not largely affect their conductivity values.[11]

The $Bi_2O_3-V_2O_5$ system has been extensively studied,[12−17] and the discovery of high ionic conductivity in BIMEVOX derivatives of $Bi_4V_2O_{11}$ has resulted in the reinvestigation of several doped phases of $Bi_4V_2O_{11}$.[18] $Bi_4V_2O_{11}$ shows a conductivity value of $\sim 10^{-1}$ S cm^{-1} at 600 °C.[19] The structure is an intergrowth between puckered bismuth oxide layers $(Bi_2O_2)^{2+}$ and perovskite blocks $(A_{n-1}B_nO_{3n+1})^{2-}$, which contain $n = 1-5$ octahedral layers.

Given that the vanadate and phosphate analogues appear isostructural, it is worth noting that the structure of the corresponding oxyphosphate $Bi_4(PO_4)_2O_3$ is not yet reported. The unit cell for the compound has been reported [ICDD (CAS: 53414-78-1)] to belong to the space group $P\bar{1}$ with $a = 7.0569(5)$ Å, $b = 9.8618(8)$ Å, $c = 15.364(2)$ Å, $\alpha = 77.648(8)°$, $\beta = 84.54(7)°$, $\gamma = 70.142(6)°$, and $V = 982.09$ Å^3. However, careful observation of the powder diffraction pattern of nominal $Bi_4(PO_4)_2O_3$ indicates the presence of more than one phase. To investigate this further, we have studied the composition range $Bi_{4+x}(PO_4)_2O_{3+3x/2}$ ($0.175 \le x \le 1$), where two new compounds were found for $x = 0.25$ and 1. The syntheses and structures of the compounds $Bi_{4.25}(PO_4)_2O_{3.375}$ and $Bi_5(PO_4)_2O_{4.5}$ are presented in this paper.

Experimental Section

Materials. Bi_2O_3 (Aldrich, 99.9%) was dried at 600 °C for 4 h before use. $(NH_4)_2HPO_4$ (SD Fine Chemicals, 99%) was used as such.

Synthesis. Polycrystalline samples of the compositions $x =$ 0.175, 0.2, 0.225, 0.25, 0.3, 0.35, 0.4, 0.45, 0.475, and 1 in the series $Bi_{4+x}(PO_4)_2O_{3+3x/2}$ ($0.175 \le x \le 1$) were synthesized by the ceramic technique. Bi_2O_3 and $(NH_4)_2HPO_4$ in stoichiometric quantities were ground well in an agate mortar. The reaction mixture was first heated at 300 °C for 3 h to expel NH_3. The resultant powder was ground well and heated at 870 °C for 3 days with intermediate grinding for compositions $x = 0.175-0.475$ and at 850 °C for 2 days for composition $x = 1$. Single crystals of both $Bi_{4.25}(PO_4)_2O_{3.375}$ and $Bi_5(PO_4)_2O_{4.5}$ were obtained by the melt−cooling technique. The pale-yellow powder of $Bi_{4.25}(PO_4)_2O_{3.375}$ was melted at 1000 °C for 1 h, cooled at a rate of 1 °C min^{-1} down to 985 °C, and then furnace-cooled to room temperature. The reaction mixture containing $Bi_5(PO_4)_2O_{4.5}$ was melted at 1170 °C for 0.5 h, cooled at a rate of 0.5 °C min^{-1} down to 900 °C, and then furnace-cooled to room temperature.

Table 1. Crystallographic Data for $Bi_{4.25}(PO_4)_2O_{3.375}$ and $Bi_5(PO_4)_2O_{4.5}$

chemical formula	$Bi_{4.25}(PO_4)_2O_{3.375}$	$Bi_5(PO_4)_2O_{4.5}$
fw	4555.1	5253.89
space group	$P\bar{1}$	$C2/c$
a (Å)	7.047(1)	13.093(1)
b (Å)	9.863(2)	5.707(1)
c (Å)	15.365(4)	15.293(1)
α (deg)	77.604(4)	90
β (deg)	84.556(4)	98.240(2)
γ (deg)	70.152(4)	90
V (Å^3)	980.90(4)	1130.95(4)
Z	4	8
T (K)	293(2)	293(2)
λ	0.710 73	0.710 73
ρ_{calc}	7.711	7.6727
μ(Mo Kα) (cm^{-1})	76.931	77.891
$R(F)^a$	0.052	0.060
$wR(F_o^2)^b$	0.103	0.1228

^{a} $R(F) = \sum||F_o| - |F_c||/\sum|F_o|$. ^{b} $wR(F_o^2) = \sum w(F_o^2 - F_c^2)^2/\sum w(F_o^2)^2]^{1/2}$.

Characterization. Powder X-ray Diffraction. Powder X-ray diffraction data of all of the phases were collected at room temperature on a Philips X'Pert Pro diffractometer, using Cu Kα radiation. Data were collected over the angular range $3° \le 2\theta \le 100°$ in steps of $\Delta(2\theta) = 0.01°$. The X-ray diffraction data were refined by a Le Bail profile analysis using the *Jana 2000*[20] program suite. The background was defined by the Chebsheyev polynomial function using 15 coefficients. The peak shapes were described by a pseudo-Voigt function with five profile parameters. For each diffraction pattern, a scale factor, a zero error factor, and shape and unit cell parameters were refined.

Differential Thermal Analysis (DTA)/Thermogravimetry. DTA measurements for the samples were performed on a SDTQ600 DSC/DTA instrument, under a constant-flow nitrogen atmosphere. There were no phase transitions and hence no weight loss observed up to 700 °C.

Single-Crystal X-ray Diffraction. Room-temperature single-crystal X-ray diffraction data were collected on a Bruker AXS SMART APEX CCD[21] diffractometer with a crystal-to-detector distance of 6.06 cm. Data were collected based on three sets of runs covering a complete sphere of reciprocal space with each set at a different φ angle ($\varphi = 0$, 90, and 180°). Each frame covered 0.3° in ω. The data were integrated using *SAINT PLUS*[21] with the intensities corrected for Lorentz and polarization. An empirical absorption correction was applied based on the cylindrical shape of the crystals. The data were solved and refined using *SHELXS97*[22] and *Jana 2000*, respectively. Crystallographic data and the details of the single-crystal data collection are given in Table 1.

ac Impedance. A circular pellet of $Bi_{4.25}(PO_4)_2O_{3.375}$ of about 10-mm thickness was sintered at 600 °C for 24 h. The compound was then sputtered with gold for ac impedance measurements. The pellet was then mounted in an impedance jig and placed in a tube furnace where the temperature was controlled to ±3 °C over the range of 30−600 °C. ac impedance measurements were carried out between 5 Hz and 13 MHz on a Hewlett-Packard HP4192A impedance gain phase analyzer. A home-built cell assembly with a two-terminal capacitor configuration and stainless steel electrodes were used for the experiment. The sample temperature was measured using a Pt−Rh thermocouple positioned very close to

(10) Mauvy, F.; Launay, J. C.; Darriet, J. *J. Solid State Chem.* **2005**, *178*, 2015.
(11) Watanabe, A.; Kitami, Y. *Solid State Ionics* **1998**, *113−115*, 601.
(12) Zhou, W. *J. Solid State Chem.* **1988**, *76*, 290.
(13) Zhou, W. *J. Solid State Chem.* **1990**, *87*, 44.
(14) Kashida, S.; Hori, T.; Nakamura, K. *J. Phys. Soc. Jpn.* **1994**, *63*, 4422.
(15) Kashida, S.; Hori, T. *J. Solid State Chem.* **1996**, *122*, 358.
(16) Watanabe, A. *Solid State Ionics* **1997**, *96*, 75.
(17) Watanabe, A.; Kitami, Y. *Solid State Ionics* **1998**, *113−115*, 601.
(18) Kendall, K. R.; Navas, C.; Thomas, J. K.; zur Loye, H.-C. *Chem. Mater.* **1996**, *8*, 642.
(19) Abraham, F.; Boivin, J. C.; Mairesse, G.; Nowogrocki, G. *Solid State Ionics* **1990**, *40/41*, 934.
(20) Petříček, V.; Dušek, M. *Jana 2000. Structure Determination Software Programs*; Institute of Physics: Praha, Czech Republic, 2000.
(21) Bruker. *SMART* (version 5.625), *SAINT* (version 6.45a), *RLATT* (version 3.0); Bruker AXS Inc.: Madison, WI, 2000.
(22) Sheldrick, G. M. *SHELXL97. Program for crystal structure refinement*; University of Göttingen: Göttingen, Germany, 1997.

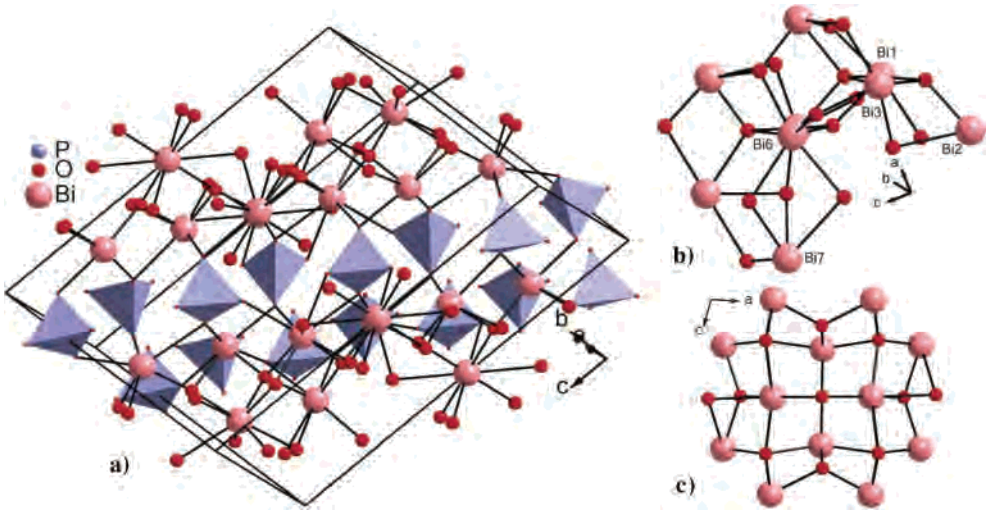

Figure 1. Crystal structure of (a) $Bi_{4.25}(PO_4)_2O_{3.375}$. Arrangement of the bismuth atoms in (b) $Bi_{4.25}(PO_4)_2O_{3.375}$ and (c) $Bi_{5.2}(MoO_4)_2O_{5.8}$.

the sample. The frequency dependence of the impedance was measured between 30 and 600 °C in a heating−cooling cycle. The samples were equilibrated for half an hour at every temperature.

Results and Discussion

Crystal Structure of $Bi_{4.25}(PO_4)_2O_{3.375}$. $Bi_{4.25}(PO_4)_2O_{3.375}$ crystallizes in the triclinic $P\bar{1}$ space group, with $a = 7.047(1)$ Å, $b = 9.863(2)$ Å, $c = 15.365(4)$ Å, $\alpha = 77.604(4)°$, $\beta = 84.556(4)°$, $\gamma = 70.152(4)°$, $V = 980.90(4)$ Å^3, and $Z = 4$ (in good agreement with the previously reported cell). The structure was solved by direct methods analysis, and the coordinates of the bismuth atoms were initially obtained. Subsequent difference Fourier syntheses revealed the remaining phosphorus and oxygen atoms in the structure. There are nine bismuth atoms in the structure. All of them occupy the general positions, except for Bi9, which occupies the 1b site. The thermal parameters of the oxygen atom O18 suggested partial occupancy, and several cycles of refinement, refining alternately the occupancy and thermal parameters, resulted in a value of 0.75(1) with acceptable thermal parameters, leading to the stoichiometry $Bi_{4.25}(PO_4)_2O_{3.375}$. Occupancy refinements of other oxygen atoms in the structure suggested full occupancy at their sites. The final R value for a total of 3142 independent reflections was 0.052. A closer examination of the unit cell parameters suggests that the structure is fluorite-related, with $a = \sqrt{2}a_F$, $b = 2a_F$, and $c = 3a_F$, where a_F corresponds to the unit cell parameter of the fluorite system. The crystal structure of $Bi_{4.25}(PO_4)_2O_{3.375}$ along the a axis consists of layers of $[Bi_9O_{19}]$ units separated by layers of isolated PO_4 tetrahedra (Figure 1a).

In $Bi_{4.25}(PO_4)_2O_{3.375}$, the repeating $[Bi_9O_{19}]$ unit consisting of Bi1−Bi9 atoms resembles a distorted "roselike" $[Bi_{12}O_{14}]$ column (Figure 1b), which is observed in phases of the type $Bi_{5.2}(MoO_4)_2O_{5.8}$[23] (Figure 1c). Each $[Bi_9O_{19}]$ unit is surrounded by seven PO_4 tetrahedra comprised of two each of $P1O_4$, $P3O_4$, and $P4O_4$ tetrahedra and one $P2O_4$ tetrahedron. The distortion in the $[Bi_9O_{19}]$ unit may be ascribed to the coordination environment around Bi2. A typical roselike column would result if Bi2 were to be connected to Bi7 and Bi6 instead of Bi1 and Bi3 (Figure 1b). A closer examination of the $[Bi_9O_{19}]$ unit (Figure 1b) clearly shows the presence of $[Bi_2O_2]$ units in $Bi_{4.25}(PO_4)_2O_{3.375}$. The formulas $Bi_{4.25}(PO_4)_2O_{3.375}$ and $Bi_{5.2}(MoO_4)_2O_{5.8}$, rewritten as $Bi_{4+x}(MO_4)_2O_{4+1.5x}$ ($x = 1.2$) and $Bi_{4+x}(PO_4)_2O_{3+1.5x}$, indicate the difference in the Bi−O ratios. The structural similarities between both of the phases are the presence of fluorite-related $[Bi_2O_2]$ units and isolated $(P/Mo)O_4$ tetrahedra. The PO_4 tetrahedra in $Bi_{4.25}(PO_4)_2O_{3.375}$ occur in layers, while the MoO_4 tetrahedra in $Bi_{5.2}(MoO_4)_2O_{5.8}$ occur in a zigzag manner.

The Bi atoms in $Bi_{4.25}(PO_4)_2O_{3.375}$ exhibit typical irregular one-sided coordination owing to the $6s^2$ lone pair of electrons on bismuth. All polyhedra containing bismuth atoms consist of five short and long Bi−O bond distances depending on the corresponding coordination geometry. The bismuth atoms exhibit varied coordination ranging from five to eight, similar to that observed in $Bi_{5.2}(MoO_4)_2O_{5.8}$.[23] Table 2a lists all of the coordination distances around each bismuth atom. Only the Bi5 atom displays all short Bi−O distances. The PO_4 tetrahedra have P−O bond distances in the range of 1.51−1.59 Å (Table 2a).

Crystal Structure of $Bi_5(PO_4)_2O_{4.5}$. The compound $Bi_5(PO_4)_2O_{4.5}$ crystallizes in a monoclinic $C2/c$ system with $a = 13.093(1)$ Å, $b = 5.707(1)$ Å, $c = 15.293(1)$ Å, $\beta = 98.240(2)°$, $V = 1130.95(4)$ Å^3, and $Z = 8$ (Table 1). The initial positions of the bismuth atoms were derived from Patterson synthesis, and subsequent difference Fourier syntheses revealed the positions of the phosphorus and oxygen atoms in the structure. The thermal parameters of the oxygen atom O7 suggested a partial occupancy, and several cycles of refinement, refining alternately the occupancy and thermal parameters, resulted in a value of 0.25(1) with acceptable thermal parameters, leading to the stoichiometry $Bi_5(PO_4)_2O_{4.5}$. All other oxygen atoms show full occupancy at their sites. The final R index for a total of 1354 independent reflections was 0.06. The structure can be related to the fluorite type as $b \approx a_F$ and $c = 3a_F$. In

(23) Vannier, R. N.; Mairesse, G.; Abraham, F.; Nowogrocki, J. *J. Solid State Chem.* **1996**, *122*, 394.

Table 2. Bond Lengths (Å) of $Bi_{4.25}(PO_4)_2O_{3.375}$ and $Bi_5(PO_4)_2O_{4.5}$

a. Bond Lengths (Å) of $Bi_{4.25}(PO_4)_2O_{3.375}$

Bi1−O1	2.30(2)	Bi2−O2	2.41(2)	Bi3−O3	2.123(19)
−O3	2.27(2)	−O9	2.26(2)	−O9	2.32(2)
−O6	2.44(2)	−O9′	2.207(18)	−O12	2.40(3)
−O9	2.45(2)	−O11	2.41(2)	−O13	2.25(2)
−O11	2.65(2)	−O13	2.77(3)	−O20	2.35(3)
−O16	2.45(2)	−O21	2.35(2)		
−O21	2.77(2)				
Bi4−O4	2.20(2)	Bi5−O1	2.08(2)	Bi6−O1	2.30(2)
−O4′	2.39(2)	−O7	2.42(2)	−O3	2.63(2)
−O5	2.65(3)	−O10	2.26(2)	−O5	2.43(3)
−O7	2.17(3)	−O15	2.32(2)	−O7	2.32(3)
−O10	2.71(2)	−O22	2.51(3)	−O8	2.71(3)
−O17	2.43(3)			−O14	2.38(5)
				−O19	2.73(3)
				−O23	2.66(3)
Bi7−O4	2.14(2)	Bi8−O3	2.43(2)	Bi9−O4 × 2	2.63(2)
−O5	2.25(2)	−O5	2.15(2)	−O7 × 2	2.53(2)
−O14	2.39(5)	−O8	2.51(2)	−O14 × 2	2.73(8)
−O17	2.63(2)	−O16	2.69(3)	−O18 × 2	2.44(3)
−O19	2.48(3)	−O22	2.56(3)		
−O23	2.39(3)				

b. Bond Lengths (Å) of $Bi_5(PO_4)_2O_{4.5}$

Bi1−O1	2.095(14)	Bi3−O1	2.225(14)
−O3	2.48(2)	−O1′	2.358(15)
−O4	2.42(3)	−O2	2.90(2)
−O5	2.28(3)	−O3	2.76(2)
−O6	2.366(19)	−O4	2.63(2)
−O7	2.56(9)	−O5	2.41(3)
Bi2−O1 × 2	2.982(15)	−O5′	2.53(3)
−O2 × 2	2.373(17)	−O6	2.61(2)
−O5 × 2	2.23(3)	−O6′	2.66(5)
−O7 × 2	2.23(8)		

$Bi_5(PO_4)_2O_{4.5}$, the bismuth atom Bi2 occupies the 2e site, while all of the other atoms occupy the general positions (8f sites). The structure of $Bi_5(PO_4)_2O_{4.5}$ (Figure 2a) along the *b* axis consists of layers of $[Bi_2O_2]$ units (Figure 2b) separated by PO_4 tetrahedra. Once again, the PO_4 tetrahedra are not interlinked in the structure. In $Bi_5(PO_4)_2O_{4.5}$, the bismuth atoms exhibit an irregular coordination (Table 2b). The PO_4 tetrahedra consist of relatively shorter P−O distances in the range of 1.47−1.58 Å.

It is noteworthy that both $Bi_{4.25}(PO_4)_2O_{3.375}$ and $Bi_5(PO_4)_2O_{4.5}$ have similar values of the unit cell parameter *c*, implying common structural features. Both of the structures are related in terms of the presence of the $[Bi_2O_2]$ units. However, a drastically different structural feature is the occurrence of partially occupied oxygen atom O18 connected to $P3O_4$ tetrahedra in $Bi_{4.25}(PO_4)_2O_{3.375}$, while in $Bi_5(PO_4)_2O_{4.5}$, the partially occupied O7 atom is connected to the Bi−O layer. The longest Bi−O bond distance in $Bi_{4.25}(PO_4)_2O_{3.375}$ is ∼2.77 Å (Table 2a), while a relatively longer distance, ∼2.90 Å (Bi3−O2), is observed in the case of $Bi_5(PO_4)_2O_{4.5}$.

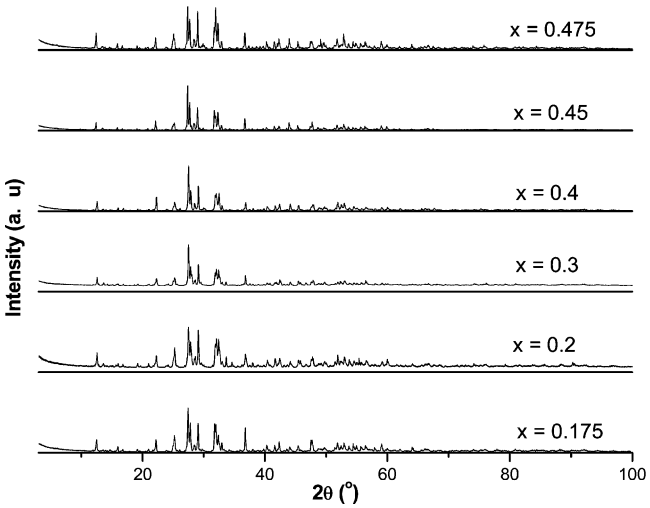

Figure 3. Powder X-ray patterns of members of the solid solution $Bi_{4+x}(PO_4)_2O_{3+3x/2}$ ($0.175 \leq x \leq 0.475$).

Structure of the Composition Range $Bi_{4+x}(PO_4)_2O_{3+3x/2}$ ($-2 \leq x \leq 1$). Figure 3 shows the powder X-ray diffraction patterns of the various compositions in the solid solution range $Bi_{4+x}(PO_4)_2O_{3+3x/2}$ ($0.175 \leq x \leq 0.475$). All of the compositions belong to the structural type $Bi_{4.25}(PO_4)_2O_{3.375}$. However, as the Bi content is decreased, the compositions show the presence of $Bi_{4.25}(PO_4)_2O_{3.375}$ as the major phase and $Bi_2(PO_4)_2$,[4] $Bi_{1.665}(PO_4)O$,[24] and $Bi_{11.5}(PO_4)_2O_{14.25}$[17] as minor phases (Figure 4). The powder X-ray diffraction patterns of $Bi_{3.5}(PO_4)_2O_{2.25}$ ($x = -0.75$) and $Bi_3(PO_4)_2O_{2.25}$ ($x = -1$) (Figure 4) indicate an increase in the percentage occurrence of the $Bi_2(PO_4)_2$ phase and a decrease in the amounts of $Bi_{4.25}(PO_4)_2O_{3.375}$ and $Bi_{1.665}(PO_4)O$. The powder pattern of $Bi_2(PO_4)_2$ ($x = -2$) has been simulated (Figure 4) from the coordinates reported by Romero et al.[4]

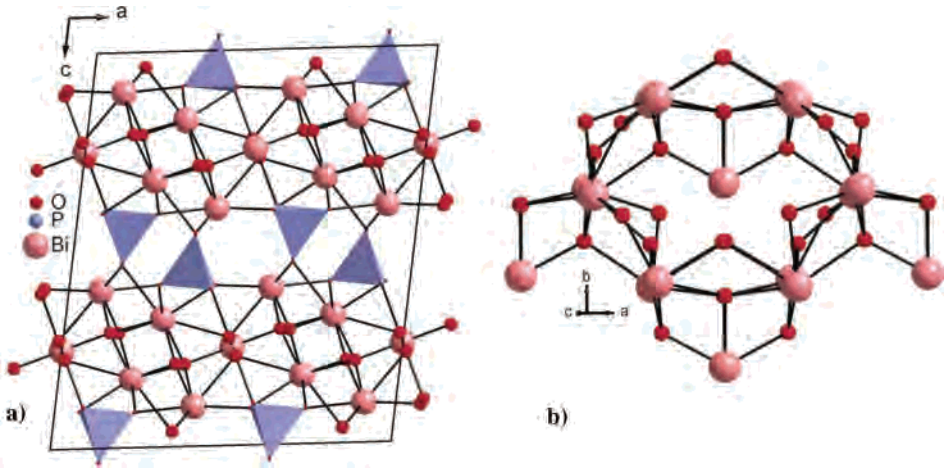

Figure 2. Crystal structure of (a) $Bi_5(PO_4)_2O_{4.5}$ and (b) arrangement of the bismuth atoms in $Bi_5(PO_4)_2O_{4.5}$.

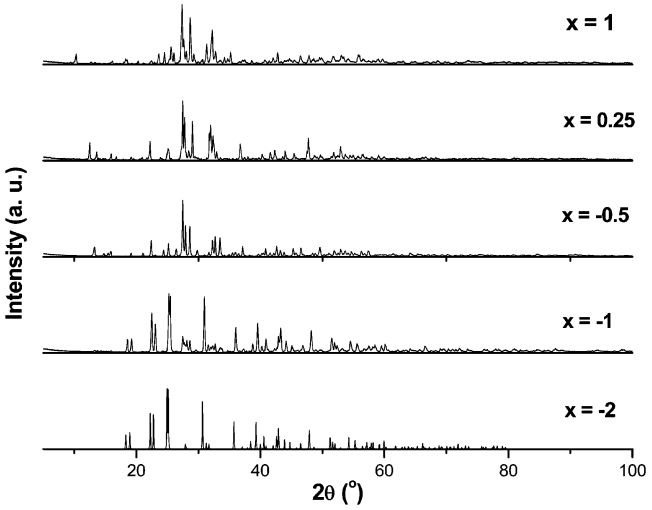

Figure 4. Powder X-ray patterns for various values of $x < 0.175$ and $x > 0.475$ in $Bi_{4+x}(PO_4)_2O_{3+3x/2}$.

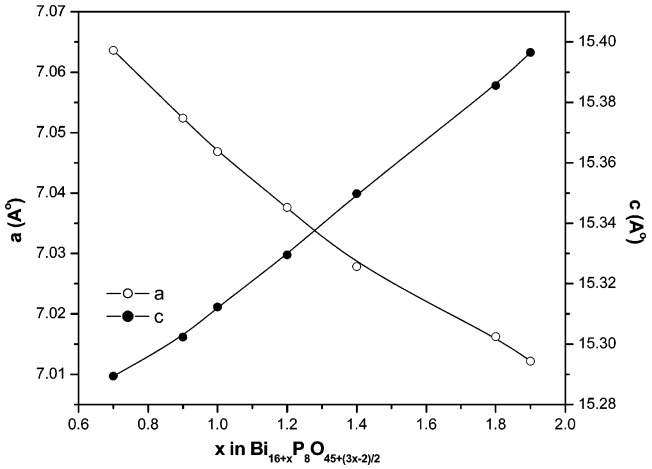

Figure 5. Variation of the unit cell parameters in the solid solution $Bi_{4+x}(PO_4)_2O_{3+3x/2}$ ($0.175 \leq x \leq 0.475$).

Compositions with $x > 0.475$ ($0.5 \leq x \leq 1$) always produce concomitant mixed phases of $Bi_{4.25}(PO_4)_2O_{3.375}$, $Bi_5(PO_4)_2O_{4.5}$, and $Bi_{11.5}(PO_4)_2O_{14.25}$ (minor phase). It may be pointed out that the synthesis of pure $Bi_5(PO_4)_2O_{4.5}$ by varying the temperature and sintering conditions was never successful because it was always contaminated with $Bi_{4.25}(PO_4)_2O_{3.375}$ and $Bi_{11.5}(PO_4)_2O_{14.25}$. The crystals of $Bi_5(PO_4)_2O_{4.5}$ could only be obtained by melting the mixed phase and identifying the resulting crystals via single-crystal X-ray diffraction. The common structural features of the impurity phases in all of the compositions are that they contain the fluorite-like $[Bi_2O_2]$ units and isolated PO_4 tetrahedra.

To establish the nature of the compositions $x = 0.175$ to 0.475 in the series $Bi_{4+x}(PO_4)_2O_{3+3x/2}$, the powder X-ray diffraction patterns were indexed. Figure 5 shows the variation of the unit cell parameters *a* and *c* with respect to composition *x*. The value of the cell dimension *b* does not vary much with composition, while *a* and *c* show opposite trends. The *a* parameter shows a decrease with an increase

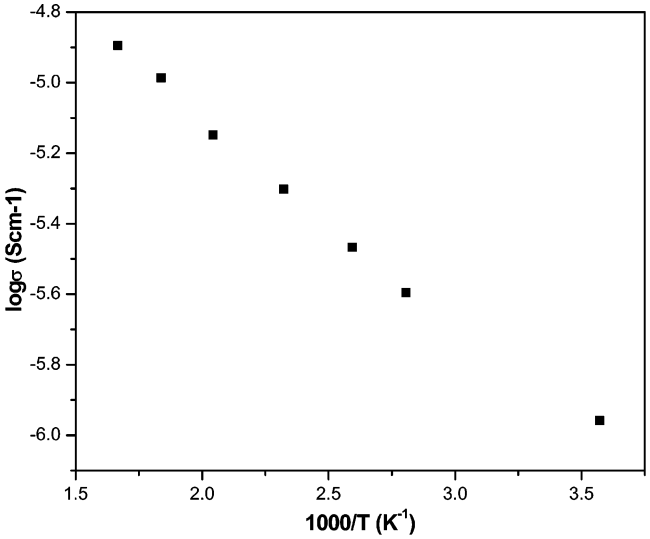

Figure 6. Conductivity Arrhenius plot of $Bi_{4.25}(PO_4)_2O_{3.375}$.

in the value of *x* in the solid solution $Bi_{4+x}(PO_4)_2O_{3+3x/2}$ in the domain $0.175 \leq x \leq 0.475$. The *c* parameter shows an increase as the bismuth content increases.

Ionic Conductivity of $Bi_{4.25}(PO_4)_2O_{3.375}$. The value of bulk ionic conductivity was calculated from the intercept of the single semicircular arcs obtained in the complex impedance plots of Z' vs Z'. $Bi_{4.25}(PO_4)_2O_{3.375}$ shows a value of 1.27×10^{-5} S cm^{-1} at 600 °C. Figure 6 shows the Arrhenius plot. As the heating and cooling cycles revealed, no change and the reported values in Figure 6 correspond to the heating cycle only. The linear behavior of log σ with $1/T$ (Figure 6) indicates the absence of any phase transition, further confirmed by DTA up to 700 °C and also confirmed by no change in the powder X-ray pattern of the sample after the conductivity measurements. $Bi_{5.2}(MoO_4)_2O_{5.8}$ shows reasonably high ionic conductivity at 600 °C (10^{-3} S cm^{-1}).[23] The conductivity mechanism was attributed to high oxygen atom exchange between the MoO_4 tetrahedra via a cooperative motion, which was found to increase with temperature.[25] In the structure of $Bi_{4.25}(PO_4)_2O_{3.375}$, the thermal parameters of the oxygen atoms in the PO_4 tetrahedra are not high as compared to the other oxygen atoms. Structures with isolated PO_4 tetrahedra have been reported to show high conductivities owing to partial occupancies of some oxygen atoms.[9,10] However, in $Bi_{4.25}(PO_4)_2O_{3.375}$, only one oxygen atom, O18, shows partial occupancy.

Conclusion

We have isolated a new series, $Bi_{4+x}(PO_4)_2O_{3+3x/2}$ ($0.175 \leq x \leq 1$), in the $Bi_2O_3-P_2O_5$ system. The composition range $0.175 \leq x \leq 0.475$ forms a solid solution. The compositions in the range $0.476 \leq x \leq 1.0$ contain $Bi_5(PO_4)_2O_{4.5}$ as the major phase and $Bi_{4.25}(PO_4)_2O_{3.375}$ as the minor phase. The crystal structures of two members of the series, $Bi_{4.25}(PO_4)_2O_{3.375}$ and $Bi_5(PO_4)_2O_{4.5}$, belong to a new structural type related to the fluorite type. The important feature in

(24) Ketatani, M.; Mentre, O.; Abraham, F. *J. Solid State Chem.* **1998**, *139*, 274.

(25) Galy, J.; Enjalbert, R.; Rozier, P.; Millet, P. *Solid State Sci.* **2003**, *5*, 165.

these structures is that both of them have isolated PO_4 tetrahedra. Further, the basic structural difference between the two compounds lies in the arrangement of the bismuth atoms. The low ionic conductivity as displayed by $Bi_{4.25}(PO_4)_2O_{3.375}$ is due to the nature of the packing of bismuth polyhedra in the crystal structure.

Acknowledgment. Single crystal X-ray data collection on the CCD facility under the IRPHA-DST program, Indian Institute of Science, is gratefully acknowledged. B.M. thanks CSIR for a senior research fellowship.

Supporting Information Available: X-ray crystallographic data in CIF format. This material is available free of charge via the Internet at http://pubs.acs.org. The crystal data for $Bi_{4.25}(PO_4)_2O_{3.375}$ and $Bi_5(PO_4)_2O_{4.5}$ have been deposited at the Fachinformationzentrum Karlsruhe (FIZ) with the numbers CSD 416043 and CSD 416044, respectively.

IC0601337